Magnetic susceptibility measurements on the mixed system cobalt nickel trimethylammonium chloride : evidence for a spin reorientation transition
by Daniel Ray Teske

A thesis submitted in partial fulfillment of the requirements for the degree of Doctor of Philosophy in Physics
Montana State University

Abstract:
Previous work on the mixed magnetic system (CH3)3NHCo1-xNixCl3.2H20 indicated a temperature versus composition phase diagram with a possible multicritical point and with low temperature regions where the system exhibits relaxation phenomena on a macroscopic time scale. A debate developed about the low temperature phase with an anisotropic spin glass model competing against a model involving domain wall dynamics.

In order to resolve questions about the nature of the low temperature regions and the conjectured multicritical point, a more complete and detailed phase diagram was needed. An extensive set of high quality crystals was grown and magnetization and magnetic susceptibility measurements were performed with better temperature control. The range of measured compositions was extended and the phase diagram near the possible multicritical point was mapped out in more detail, resulting in the discovery of a previously unresolved phase transition curve. The newly discovered phase transition curve is attributed to spin reorientation. The qualitative shape of the phase transition lines is explained in terms of the crossing of free energy curves and a Landau theory having an order parameter with two components is proposed.

MAGNETIC SUSCEPTIBILITY MEASUREMENTS ON THE MIXED SYSTEM COBALT NICKEL TRIMETHYLAMMONIUM CHLORIDE: EVIDENCE FOR A SPIN REORIENTATION TRANSITION

by

Daniel Ray Teske

A thesis submitted in partial fulfillment
of the requirements for the degree

of

Doctor of Philosophy

in

Physics

MONTANA STATE UNIVERSITY-BOZEMAN
Bozeman, Montana

January 1998

APPROVAL

of a thesis submitted by

Daniel Ray Teske

This thesis has been read by each member of the thesis committee and has been found to be satisfactory regarding content, English usage, format, citations, bibliographic style, and consistency, and is ready for submission to the College of Graduate Studies.

Dr. John E. Drumheller _____ (Signature) 1/16/98 Date

Approved for the Department of Physics

Dr. John Hermanson _____ (Signature) 1-16-98 Date

Approved for the College of Graduate Studies

Dr. Joseph J. Fedock _____ (Signature) 1/20/98 Date

STATEMENT OF PERMISSION TO USE

In presenting this thesis in partial fulfillment of the requirements for a doctoral degree at Montana State University-Bozeman, I agree that the Library shall make it available to borrowers under rules of the Library. I further agree that copying of this thesis is allowable only for scholarly purposes, consistent with "fair use" as prescribed in the U.S. Copyright Law. Requests for extensive copying or reproduction of this thesis should be referred to University Microfilms International, 300 North Zeeb Road, Ann Arbor, Michigan 48106, to whom I have granted "the exclusive right to reproduce and distribute my dissertation in and from microform along with the non-exclusive right to reproduce and distribute my abstract in any format in whole or in part."

Signature Daniel Teske

Date Jan. 16, 1998

This thesis is dedicated to E. M. Kessler.

ACKNOWLEDGMENTS

I would like to thank my advisor, Professor John E. Drumheller, for his unwavering support, both material and moral. I would also like to thank Dr. D. Haines and Dr. S. Lanceros-Méndez for their considerable help.

TABLE OF CONTENTS

TABLE OF CONTENTS-continued

LIST OF TABLES

LIST OF FIGURES

LIST OF FIGURES-continued

LIST OF FIGURES-continued

Figure page

ABSTRACT

Previous work on the mixed magnetic system $(CH_3)_3NHCo_{1-x}Ni_xCl_3 \cdot 2H_2O$ indicated a temperature versus composition phase diagram with a possible multicritical point and with low temperature regions where the system exhibits relaxation phenomena on a macroscopic time scale. A debate developed about the low temperature phase with an anisotropic spin glass model competing against a model involving domain wall dynamics. In order to resolve questions about the nature of the low temperature regions and the conjectured multicritical point, a more complete and detailed phase diagram was needed. An extensive set of high quality crystals was grown and magnetization and magnetic susceptibility measurements were performed with better temperature control. The range of measured compositions was extended and the phase diagram near the possible multicritical point was mapped out in more detail, resulting in the discovery of a previously unresolved phase transition curve. The newly discovered phase transition curve is attributed to spin reorientation. The qualitative shape of the phase transition lines is explained in terms of the crossing of free energy curves and a Landau theory having an order parameter with two components is proposed.

CHAPTER 1

INTRODUCTION

Motivation

The temperature versus composition phase diagram of the quasi one-dimensional canted antiferromagnet $(CH_3)_3NHCo_{1-x}Ni_xCl_3 \cdot 2H_2O$ exhibits a number of interesting features including a possible multicritical point, a transition due to spin reorientation, metamagnetic domain formation and transition temperatures for material compositions near $x = 0.5$ which are higher than those of the end members at $x = 0$ and $x = 1$. Prior to this work the multicritical point had not been experimentally studied in any great detail and the transition due to spin reorientation had not been seen before. This mixed compound presents the opportunity to study spin reorientation in a system for which some of the governing parameters can be varied by changing the Ni / Co ratio. Relaxation phenomena vary considerably with composition in this material and the debate over the nature of these phenomena has recently received an infusion of new information from neutron scattering [1] and NMR [2] experiments. For $0 < x < 1$ the system is assumed to be site disordered and it is unusual for magnetic transition temperatures to increase with increasing disorder.

This mixed magnetic system presents a variety of phenomena at easily accessible temperatures.

Nomenclature

A number of abbreviations are used to refer to $(CH_3)_3NHCo_{1-x}Ni_xCl_3 \cdot 2H_2O$. The organic salt trimethylammonium chloride which has the formula $(CH_3)_3NHCl$ is abbreviated as TAC. In some of the earliest literature the abbreviation TMA was used. The mixed composition family is usually referred to as CoNiTAC with the end members being called CoTAC and NiTAC. To refer to a specific intermediate composition, one can write $Co_{1-x}Ni_xTAC$.

Properties Common to CoTAC and NiTAC

As with any mixed system, it is important to understand as much as possible about the pure materials. This is particularly true of CoNiTAC because a number of experiments have indicated that many of its properties, for example the canting angle, can be computed to good approximation as the compositional average of the corresponding properties of the two pure systems CoTAC and NiTAC.

CoTAC and NiTAC are structurally isomorphous and have similar magnetic behavior. Both are orthorhombic and belong to the space group Pnma with magnetic space group Pnm'a' at zero field [1]; however, for CoTAC at least, the groups Pn'm'a and Pnm'a' are estimated to be separated by an energy on the order of only 10^{-3} K and for

applied fields greater than 64 Oe for CoTAC, the group Pn'm'a is thought to be relevant for parts of the crystal [3]. The three-dimensional ordering is antiferromagnetic for both CoTAC and NiTAC but these are quasi-one-dimensional materials with chains of bichloride bridged metal ions having strong ferromagnetic coupling along the chains. Figure 1 shows the unit cell (not all spins are shown, not all Cl^- ions are shown and the $(CH_3)_3NH^+$ groups are not shown). The metal ions are octahedrally coordinated with four chloride ions and two water molecules. Figure 2 emphasizes the spins. There are two kinds of magnetically inequivalent chains [4].The chains run in the crystallographic **b** direction and **bc** planes of chains are separated in the **a** direction by $(CH_3)_3NH^+$ groups. Referring again to Fig. 2 we see that the spins point nearly in the **c** direction with canting towards the **a** direction and there are two antiferromagnetic sublattices. The **c** components of the spins of the two sublattices cancel, resulting in the antiferromagnetic behavior in the **c** direction but the relatively smaller **a** components combine to give weak ferromagnetism along the **a** axis. The hard axis is in the **b** direction and although strictly speaking the easy axis is different for the two sublattices, the **c** axis is referred to as the easy axis. It is important to relate this to crystal morphology. The crystals are elongated in the **b** direction and the vast majority have wedge shaped ends. The edge of each of the two end wedges lies along the **a** direction. The following gives some further quantitative comparisons which are summarized in Table 1.

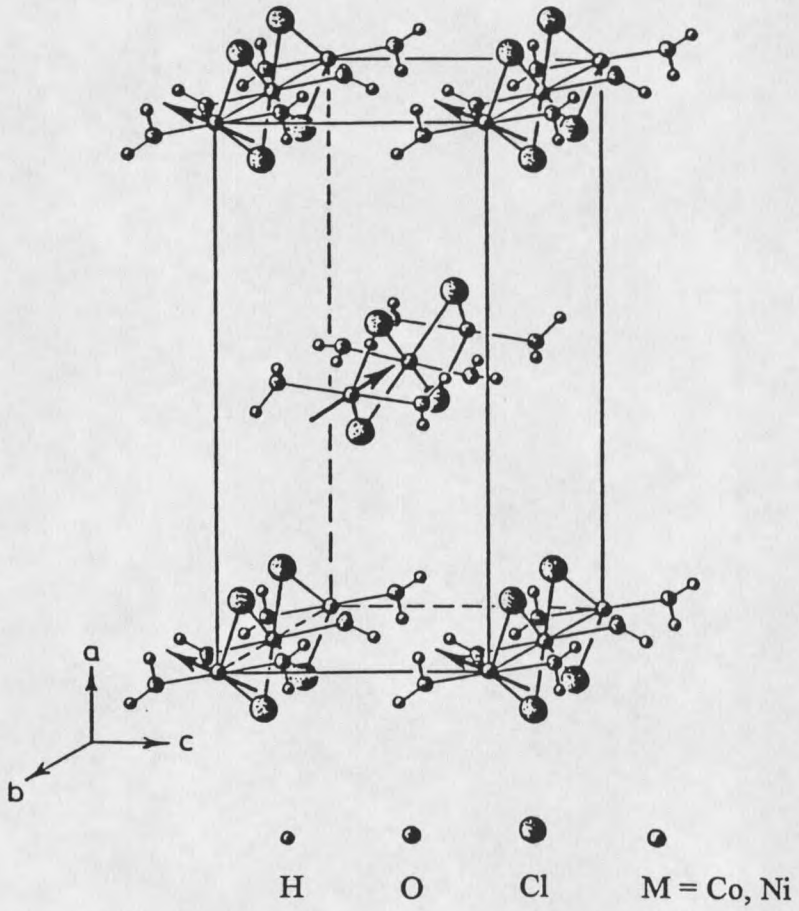

FIG. 1. Coordination of metal ions in MTAC, M = Co, Ni. Not all atoms of the crystal structure are shown and not all spins are shown. After [6].

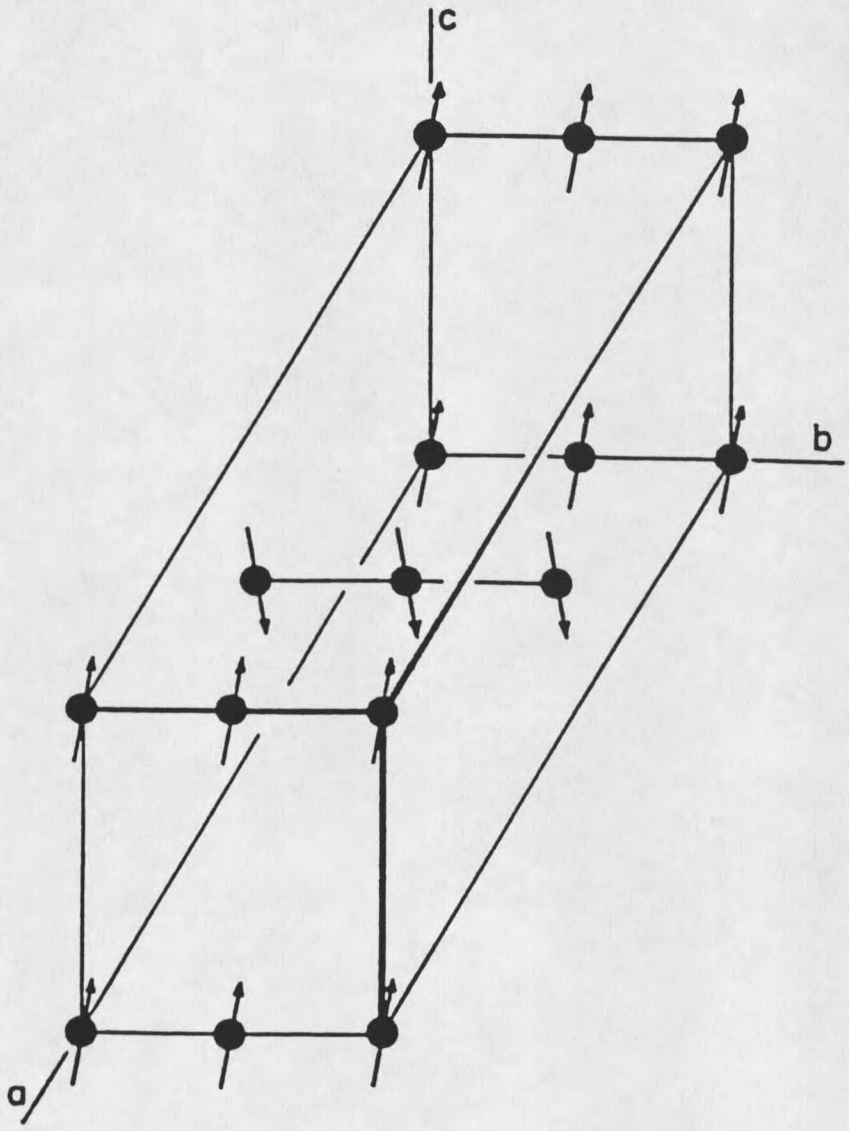

FIG. 2. Spin arrangement of MTAC, M = Co, Ni at T = 0 K and zero applied magnetic field. After [3].

		CoTAC	NiTAC
	T_c (K)	4.14	3.67
	spin	3/2	1
lattice	a (Å)	16.671(3)	16.677(5)
constants	b (Å)	7.273(1)	7.169(2)
	c (Å)	8.113(2)	8.103(2)
exchange	J_b/k (K)	13.8	14
coupling	z_cJ_c/k (K)	0.28	0.13
constants	z_aJ_a/k (K)	-0.032	-0.024
g	g_a	3.1	
	g_b	3.8	
	g_c	7.5	2.25
	canting angle	10°	21°

Table 1. Parameter values for CoTAC and NiTAC. The values of the exchange constants and g values should be considered as estimates only.

Specific Properties of CoTAC

CoTAC is a spin 3/2 system. A $3d^7$ ion such as Co(II) has the spectroscopic symbol $^4F_{9/2}$ and this F-state is split by an octahedral field to give a ground state having 3-fold orbital degeneracy. For CoTAC the orbital angular momentum is effectively quenched and the spin degeneracy is also lifted, resulting in a Kramer's doublet ground state. CoTAC orders antiferromagnetically at 4.14 K. The lattice constants (presumably determined at room temperature) [5] are a = 16.671(3) Å, b = 7.273(1) Å and c = 8.113(2) Å. The crystal contains chlorobibridged chains of ferromagnetically coupled Co(II) ions running along the **b** direction. The exchange couplings and g values were estimated [6] using a 1-D Ising model with a mean-field correction. The Hamiltonian for a one-dimensional Ising system can be written as

$$\mathcal{H} = -2J_b \sum_i^N S_i^z S_{i+1}^z - g\mu_B H \sum_i^N S_i^z \qquad (1)$$

where J_b is the exchange interaction ($J_b > 0$ is ferromagnetic) and S^z_i equals $\pm 1/2$ (for CoTAC, as shown in Fig. 1, half of the chains have one principal axis and half have another so the **z** axis referred to in Eq. 1 is different for the two magnetically inequivalent types of chains). Mean-field approximations gave information about the exchange couplings and g values perpendicular to the chain. Reported were an intrachain coupling of J_b/k = 13.8 K and interchain interactions z_cJ_c/k = 0.28 K and z_aJ_a/k = -0.032 K. The estimated g values were g_c = 7.5, g_b = 3.8 and g_a = 3.1 which are consistent with the

assumption that this is a good approximation to an Ising system. The canting angle for CoTAC is 10° off the **c** axis and towards the **a** axis [1, 3].

Specific Properties of NiTAC

NiTAC is a spin 1 system. A $3d^8$ ion such as Ni(II) has the spectroscopic symbol $^3F_4$ and this F-state is split by an octahedral field to give an orbital singlet ground state. For NiTAC the single-ion anisotropy lifts the spin degeneracy resulting in a spin singlet low. The magnetic properties are due to the nearby $S^z = \pm 1$ doublet. NiTAC orders antiferromagnetically at 3.67 K. The lattice constants are a = 16.677(5) Å, b = 7.169(2) Å and c = 8.103(2) Å. The crystal contains chlorobibridged chains of ferromagnetically coupled Ni(II) ions running along the **b** direction. A Hamiltonian for a spin 1 magnetic chain in NiTAC [4] can be written as

$$\mathcal{H} = -2J_b \sum_i^N \vec{S}_i \cdot \vec{S}_{i+1} - D \sum_i^N \left(S_i^z\right)^2 - E \sum_i^N \left(\left(S_i^x\right)^2 - \left(S_i^y\right)^2\right)$$

$$- g\mu_B H_o \sum_i^N S_i^z + \mathcal{H}_{int} \qquad (2)$$

where J_b is the intrachain exchange ($J_b > 0$ is ferromagnetic), D is the uniaxial single-ion anisotropy, E is the orthorhombic component of the single-ion anisotropy, H_o is the external magnetic field and $\mathcal{H}_{int}$ includes the exchange and dipolar interactions between the chains (for NiTAC, as shown in Fig. 1, half of the chains have one principal axis and half have another so the **z** axis referred to in Eq. 2 is different for the two magnetically

inequivalent types of chains). There has been some doubt expressed as to the appropriate Hamiltonian to apply. The g values are temperature dependent with the system going from Ising-like to easy plane behavior as the temperature increases from 10 to 15 K. Also the single-ion anisotropy has a significant orthorhombic component. Nevertheless, de Neef's model [7] for an S =1 ferromagnetic chain with uniaxial single-ion anisotropy was applied to estimate g and the intrachain exchange. The values reported [4] were J_b/k = 14 K and g = 2.25. Application of mean field theory gave estimates z_fJ_f/k = 0.13 K and $z_{af}J_{af}/k$ = -0.024 K (z_f = 2 and z_{af} = 4) for the interchain exchange constants. Referring to the **a** and **c** axes of the crystal, $J_a = J_{af}$ and J_c is essentially equal to J_f. The canting angle for NiTAC is 21° off the **c** axis and towards the **a** axis.

Density

In order to easily determine the volume of a sample it is useful to know its density. It will sometimes be convenient to work with volume susceptibility so we need to know the density of $Co_{1-x}Ni_xTAC$. The density can be calculated from the lattice parameters determined from x-ray data. The molecular weights of cobalt and nickel are very close with values 129.84 g/mole for cobalt and 129.62 g/mole for nickel. As can be seen from Table I, the lattice parameters of CoTAC and NiTAC are also very close. Since we are interested in the behavior at low temperature, the lattice parameters determined at 4 K [1] will be used. Those parameters are a = 16.490(11) Å, b = 7.209(3) Å, and c = 7.957(4) Å

and refer to the unit cell shown in Fig. 1. There are four formula units per unit cell and the formula weight of CoTAC is 261.44 g/mole. The density is

4(mass of one formula unit)/(unit cell volume) = 1.836 g/cm^3.

The lattice parameters at 4 K for $Co_{0.41}Ni_{0.59}$TAC have also been determined [1]. Using those values, a density of 1.818 g/cm^3 is calculated. In the work which follows a value of 1.82 g/cm^3 will be used as the approximate density of $Co_{1-x}Ni_x$TAC at intermediate values of x.

Units

A review of Gaussian and electromagnetic units follows. One can easily convert from one system to the other by realizing that the symbol emu is equivalent to units of cm^3. In Gaussian units the magnetic moment per unit volume M and the magnetic field H both have units of Oe. The volume susceptibility χ is determined by $M = \chi H$ and therefore χ is dimensionless. In electromagnetic units, M and H still both have units of Oe but the dimensions of χ are written as emu/cm^3. Because of this awkward notion of using the abbreviation emu to stand for cm^3, it is easier in practice to think in terms of Gaussian units. In Gaussian units, the magnetic moment per unit mass is M/density so it has units of Oe·cm^3/g and the magnetic moment per mole is M(mol. wt./density) so it has units of Oe·cm^3/mol. The mass susceptibility χ_{mass} and the molar susceptibility χ_{molar} are defined so that $\chi_{mass}H$ equals the magnetic moment per unit mass and $\chi_{molar}H$ equals the magnetic moment per mole. Therefore the units of χ_{mass} are cm^3/g and the units of χ_{mol} are cm^3/mol.

As an example, the units of χ_{mass} in the electromagnetic system of units would be specified as emu/g.

Demagnetization Factor

Demagnetizing effects are significant for samples with large susceptibilities. For CoNiTAC, large susceptibilities occur along the **a** and **c** axes. Let us denote the externally applied magnetic field by H_o, the internal magnetic field by H_i and the magnetization by M. The demagnetization factor N_{jk} is a tensor, but if the magnetic field is applied along a principal axis and the diagonal element of N_{jk} corresponding to this axis is denoted by N, then

$$H_i = H_o - NM \qquad (3)$$

In order for H_i to be uniform, the sample should be ellipsoidally shaped. The demagnetization factor can be calculated for an ellipse [17] and can be estimated for reasonably simple shapes. For nonellipsoidal shapes the internal field will be nonuniform and hence the demagnetizing effect will be nonuniform. The demagnetization effect depends on the shape of the sample and it can also depend on domain structure [18].

Metamagnets

It is worthwhile to review the concept of a metamagnet since both CoTAC and NiTAC are metamagnets and experiments thus far indicate that for any x, $Co_{1-x}Ni_xTAC$ is also. Metamagnets are highly anisotropic antiferromagnets which can at low temperature

undergo a field-induced first order phase transition from the antiferromagnetic state to a state having relatively high magnetization. This transition is characterized on the microscopic scale by a reversal of some of the spins (large anisotropy constrains the spins to lie along or very nearly along the easy axis) [8]. This is in contrast to a nearly isotropic antiferromagnet where a considerably less than 180° rotation (i.e. spin flop) is seen. Figures 3 and 4 show schematic phase diagrams for a metamagnet, and for comparison, Fig. 3 also shows a schematic phase diagram for an isotropic antiferromagnet. For the low temperature transition to be first order there must be competing interactions [8,9] which for a metamagnet means a competition between ferromagnetic and antiferromagnetic interactions. If one starts with an appropriate expression for the internal energy involving parameters for the competing interactions and determines M versus H, then for certain regions of parameter space, the antiferromagnetic solution can be multiple-valued with portions of unstable values. In that case, as H increases the system eventually goes from the antiferromagnetic to a paramagnetic or ferrimagnetic state; however the system will not traverse the unstable portion in the M versus H diagram. Instead the magnetization will change discontinuously which of course indicates a first order transition. It should be emphasized that there can also be regions of parameter space for which the transition is second order.

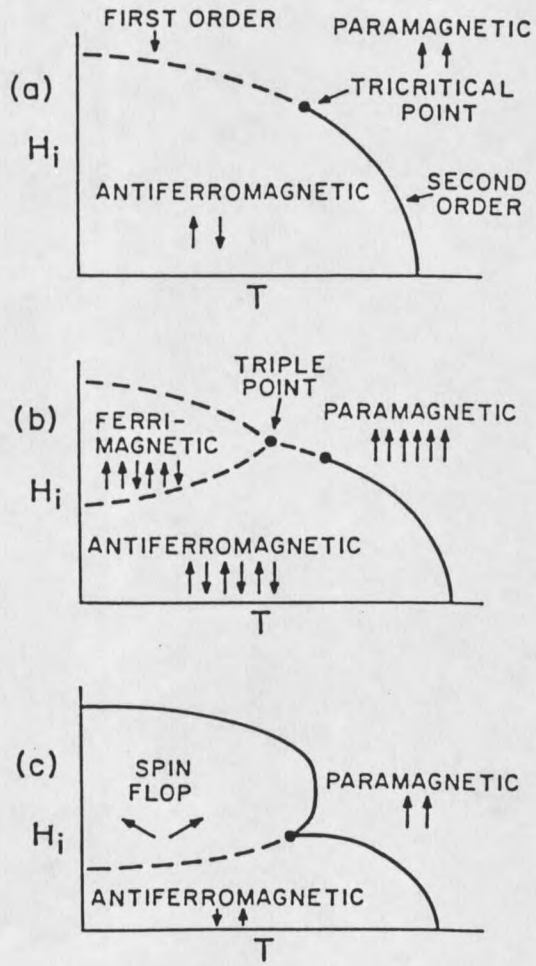

FIG. 3. Schematic phase diagram of the internal magnetic field H_i versus temperature T for (a) a metamagnet of the same type as CoTAC or NiTAC, (b) a metamagnet that has a ferrimagnetic phase, (c) an isotropic antiferromagnet. After [8].

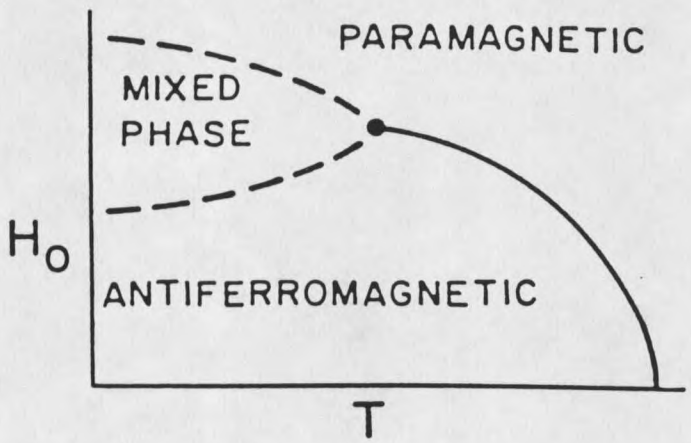

FIG. 4. Schematic phase diagram of the applied magnetic field H_o versus temperature T for a metamagnet of the same type as CoTAC or NiTAC. After [8].

Multicritical Points

Thermodynamic quantities describe the macroscopic state of a system. Examples of these quantities are P, V, T, U, fractional concentration x, etc. For a system of identical particles, only two thermodynamic quantities are needed to specify the state of the system. For an N component system, N + 1 thermodynamic quantities are needed. Usually all but two of the quantities are held constant and the graph of the remaining two free variables constitutes a phase diagram. A curve separating two phases that are in equilibrium is called a phase equilibrium curve. A point where two or more phase equilibrium curves intersect is called a multicritical point. By convention, the name of a specific type of multicritical point contains implicit information. For example, a tetracritical point is not simply a point where four phase equilibrium curves meet. That condition is required and in addition, all four curves must correspond to a second order transition. The various phase diagrams of CoNiTAC have multicritical points. It has been conjectured that the temperature versus composition phase diagram of CoNiTAC exhibits a tetracritical point. Since $Co_{1-x}Ni_xTAC$ is a metamagnet of the mixed phase type, the applied field H_o versus T phase diagram with the field oriented along the easy axis has a multicritical point.

Summary of Previous Work on CoNiTAC

Early studies of CoTAC [3,5,6,10] and NiTAC [4,11,12] demonstrated their interesting magnetic properties and many similarities. Since the two materials are not only structurally isomorphous but also have lattice constants which are close in value, it is not

surprising that they can form mixed crystals for all values of composition. Initial work on CoNiTAC [13,14,15] determined an interesting temperature versus composition phase diagram. Based primarily on measurements of thermoremanent magnetization, the low temperature phase was modeled as an anisotropic spin glass and evidence for a multicritical point was observed. Subsequent neutron scattering [1,16] and NMR [2] experiments disproved the spin glass model and showed that, as is the case for CoTAC and NiTAC, the low temperature phase of $Co_{1-x}Ni_xTAC$ is a canted antiferromagnet with macroscopic dynamics attributed to domain wall motion. This thesis will show that for $0.1 < x < 0.6$, $Co_{1-x}Ni_xTAC$ has two ordered phases, both being canted antiferromagnets but with different canting angles.

CHAPTER 2

EXPERIMENTAL RESULTS

Objective

The objective of the experiments was to map out more completely the temperature versus composition phase diagram of CoNiTAC. All but one of the magnetic measurements for the original work on the phase diagram [13,14] were performed using powdered samples measured in an EG&G PAR model 155 vibrating sample magnetometer. One small crystal was measured using an AC SQUID system. Since $Co_{1-x}Ni_xTAC$ is highly anisotropic, single crystal data were obviously needed in order to get a more detailed phase diagram. AC susceptibility measurements are advantageous because, unlike magnetization measurements, they can be done at essentially zero applied field except for an ac excitation field on the order of one Oe or less. This is particularly important for the study of a material like CoTAC which has a critical field at 65 Oe.

Crystal Growing Techniques

Crystals of $(CH_3)_3NHCo_{1-x}Ni_xCl_3 \cdot 2H_2O$ can be grown by slow evaporation of an aqueous solution containing a 1-1 molar ratio of magnetic ions to trimethylammonium

ions. Since the cobalt, nickel and trimethylammonium chlorides are all highly soluble in water, the solutions tend to become extremely concentrated before crystallization begins and some techniques were required to prevent the crystallization from occurring too rapidly since extremely rapid crystallization generally results in a large number of small, poor quality crystals. The following describes the crystal growing procedure.

The chlorides $NiCl_2 \cdot 6H_2O$, $CoCl_2 \cdot 6H_2O$ and $(CH_3)_3NHCl$ were used. It should be noted that $NiCl_2$, $CoCl_2$ and their various hydrates are toxic and cancer suspect agents and that $CoCl_2 \cdot 6H_2O$ is a possible sensitizer. Glass sample bottles with plastic caps were used to grow the crystals. For a given Ni-Co ratio, an aqueous solution was made having a 1-1 molar ratio of magnetic ions to trimethylammonium ions and having only enough water added to just dissolve the chlorides. The solution was divided equally between 5 or more sample bottles with a solution depth greater than 2.5 cm in each. The water was allowed to evaporate and as crystallization just began in each container, it was sealed with the plastic cap. After visual inspection, one of the containers was selected to provide seed crystals. The crystals from that container were removed, washed with 95% ethanol, air dried and stored in a sealed container. The trimethylammonium ion is relatively heat stable so the solutions can withstand gentle heating. For each remaining container, a drop or two of water was added and the open container was heated with a hotplate until the bottom of the glass was hot to the touch. This was always sufficient to dissolve all of the crystals. Upon removal from the hotplate the container was again temporarily sealed to avoid excessive evaporation during cooling. While the solution was cooling, a seed crystal was

selected from the crystals collected earlier. The seed was placed in a crease of a piece of tissue paper (the tissue was used in order to make retrieval of the seed easier) and washed in 95% ethanol for one to three minutes depending on its initial size. The washing was necessary to smooth the surface of the seed and to dissolve away any structurally weak fragments that could break off and serve as nucleation sites. Next the seed was added to the now cooled solution and the container was again sealed with the plastic cap. If the right number of drops of water was added, the seed would begin to grow along with several other crystals. The one from the seed is often defective since any structural defects in the seed will tend to be preserved as it grows, but the others can be quite good. When collected, the crystals can be washed with 95% ethanol and then air dried thoroughly before storage in a sealed bottle. The crystals should not be stored with a desiccant because that causes them to lose water of hydration.

As the Ni concentration in solution changes from 0 to 100%, the ease of growing crystals varies. It is easy to grow pure CoTAC or mixed crystals in a range from 35 to 45 atomic % Ni in solution or for a narrow range near 90% Ni in solution. NiTAC is by far the most difficult and takes months to grow. In order to obtain seeds for NiTAC, the temperature of the solution had to be raised several degrees above room temperature. That probably means room temperature is not optimal for growing NiTAC. An attempt to find the optimal temperature was not pursued. In the literature it has been mentioned that lowering the pH of the NiTAC solution with HCl will result in larger crystals [11]. That technique was not applied to the NiTAC crystals grown for this work. They were grown

under conditions of temperature and pH that were the same as the conditions of growth for the mixed crystals.

Crystal Morphology

As previously noted, the crystals are elongated with almost all of them having wedge shaped ends. When normal CoNiTAC crystals are viewed end on, the cross section perpendicular to the long axis can be approximately described as a rhombus (diamond shaped) with the edge of the end wedge along a diagonal. The cross section is not quite a rhombus because two of the "vertices" are really very short edges corresponding to two narrow facets of the crystal so the cross section really looks like a rhombus with two of its vertices shaved off. The **a**-axis of the crystal, which is the axis of weak ferromagnetism, is in the direction along the edge of the end wedge. That direction is usually consistent from end to end although a few crystals showed a slight twisting about the long axis. The **b**-axis, which is the hard axis, is along the elongated dimension. A small percentage of the crystals had end wedges that were significantly distorted or the wedges were nonexistent. Their cross sections perpendicular to the long axis tended to be rectangular. These crystals were found to have different orientation properties than the normal crystals.

Some idea of the quality of a crystal can be obtained by observing it with polarized light. $Co_{1-x}Ni_xTAC$ exhibits optical dichroism with the phenomenon being particularly striking at intermediate concentrations.

Instrumentation

Magnetic susceptibility and magnetization measurements were performed using a 7225 Lake Shore Susceptometer/Magnetometer. Details about the machine and its operation can be found in the 7000 Series AC Susceptometer / DC Magnetometer User's Manual. Susceptibility and temperature calibration were checked with Pb and Ga. For temperatures between 3 and 10 K the temperature sensor at the sample was estimated to be systematically reading 0.02 K too low. The susceptibility was reading too large in magnitude by approximately 3%.

The sensitivity of the 7225 AC Susceptometer is a result of the design and fabrication of the primary and secondary coils, the minimization of eddy currents and the design of the superconducting magnet. The secondary coils, which consist of two coils wound in opposition, are well balanced, have a large number of turns and are strongly coupled to the sample space [19]. The primary coil is uniformly wound and is long relative to the secondary. Eddy currents have been kept to a minimum by using nonconductive materials in the vicinity of the coils. The superconducting magnet has been designed to minimize inductive coupling to the coils. The manual specifies the AC sensitivity to be "To 2×10^{-8} emu in terms of equivalent magnetic moment". This means that a change in moment Δm can be resolved to this level, where

$$\Delta m = (\Delta M)(V), \qquad (4)$$

V is the sample volume and ΔM is the change in magnetization of the sample. Another way to think about this is to examine the relation

$$\chi \cong \frac{\Delta M}{\Delta h} = \frac{\Delta m}{V \Delta h} \tag{5}$$

where Δh is the change in the applied magnetic field. In order to resolve the signal from noise, we need to have

$$|\chi| \geq \frac{2 \times 10^{-8}}{V \Delta h} \tag{6}$$

There are several reasons why simply increasing the sample volume V or the ac excitation field Δh is not the answer to every problem. Obviously the volume is constrained by the size of the sample space. The coupling of the coils to the sample depends an sample volume so the appropriate calibration constant for the coils depends slightly on sample volume. Usually the ac excitation field should be set as low as possible while still obtaining a good signal to noise ratio. The highest excitation field available on the 7225 is 25.1 Oe. If one is interested in phenomena at zero applied field, then an excitation field of that order is a significant violation of a zero field condition. Also, as Δh increases so does the offset voltage. If the offset voltage dominates the signal voltage, the sensitivity is compromised. The offset voltage also increases nonlinearly with increasing frequency due to capacitive and inductive effects, so for high frequency operation it is particularly important to keep Δh as small as possible. The highest sensitivities are achieved for frequencies between approximately 100 and 1000 Hz. With careful selection of Δh for a given frequency, sensitivities of 10^{-9} emu or better can be achieved [19].

A rough check of susceptibility calibration can be done by measuring the susceptibility of a zero field cooled piece of Pb shot. If we assume the piece of shot is spherical, then in electromagnetic units (emu) the demagnetization factor is $4\pi/3$ and for T well below the superconducting transition temperature the susceptibility is $-1/4\pi$. This follows because

$$H = B - 4\pi M \tag{7}$$

and for a type I superconductor such as Pb, if the applied field H_o is less than the critical field, then the Meissner effect results in $B = 0$ well inside the superconductor. In other words, supercurrents flow on the surface of the sphere so that in the interior,

$$H_i = -4\pi M. \tag{8}$$

From this we see that

$$\frac{dM}{dH_i} = \frac{-1}{4\pi} \tag{9}$$

where

$$\chi = \frac{dM}{dH_i} \tag{10}$$

is the volume susceptibility. [The volume susceptibility is dimensionless. In the electromagnetic system of units however, the volume susceptibility is specified as χ (emu/cm^3).] So far we have not seen the demagnetization factor come explicitly into play. It becomes involved because, in measuring the effect of a changing field on a sample we are dealing with a boundary value problem. The external applied field H_o is of course

not generally the same as the internal field H_i. The hardware only knows what the measured susceptibility

$$\chi_m = \frac{dM}{dH_o} \tag{11}$$

is, but for the purposes of theory we are really interested in χ given by Eq. 10.

In order to determine χ from χ_m values, the demagnetization factor must be known. The demagnetization factor is a tensor which depends on the shape of the sample as well as its composition. For a sample of arbitrary shape the demagnetization factor can vary with position within the sample, but for an ellipsoid, the tensor is the same throughout the sample [17]. The situation is particularly simple for a sphere where for an isotropic sample, any axis can be taken as a principal axis. To get an idea of how to determine the demagnetization factor of a sphere, consider from the point of view of a boundary value problem, a superconducting sphere placed in an external field H_o. If we assume that the Meissner effect will result in the sphere being uniformly magnetized we can get a consistent set of solutions for inside and outside the sphere which agree with experimental results. The solution for the case of a uniform field $B_o = H_o$ through all space superposed on the field of a uniformly magnetized sphere is [20]

$$B_i = B_o + (8\pi/3)M \tag{12}$$

$$H_i = B_o - (4\pi/3)M. \tag{13}$$

But $B_o = H_o$ so in this case

$$H_i = H_o - (4\pi/3)M. \tag{14}$$

Recalling that the demagnetization factor N is determined by Eq. 3, we see that $N = 4\pi/3$ for a sphere. If the correct demagnetization factor is entered into the Lake Shore data analysis program, χ will be calculated from the measured value χ_m and then the graphical output will display χ. Again using Eq. 3

$$\frac{dH_i}{dM} = \frac{dH_o}{dM} - N \tag{15}$$

$$\frac{1}{\chi} = \frac{1}{\chi_m} - N \tag{16}$$

$$\chi = \frac{1}{\frac{1}{\chi_m} - N} = \frac{\chi_m}{1 - N\chi_m} \tag{17}$$

The value of N can be entered at the time of data acquisition in which case it will become the default value for that data file or the value of N can be interactively changed during data analysis of a given file. Note that if N is set to zero, then χ_m will be displayed. For a superconducting sphere the theoretical value for χ is $-1/4\pi$, but unless one supplies the software with the correct demagnetization factor, that is not what the output will show.

Volume susceptibility χ versus temperature T for a Pb sphere is shown in Fig. 5. No attempt was made to eliminate the surface oxidation. Ideally the Pb shot is washed for a short time with nitric acid to remove oxidation and smooth the surface. Since we wanted to use the same sphere for each test, the washing was not done because it would have eventually consumed the sphere. As can be seen in Fig. 5, the value of susceptibility is slightly more negative than $-1/4\pi = -0.0796$. This sample was also used to check the consistency of the thermometry. For the 99.7% pure Pb sphere of mass 0.0104 g which